Journal of Materials Chemistry B

Accepted Manuscript

ROYAL SOCIETY OF CHEMISTRY

www.rsc.org/materialsB

Cite this: DOI: 10.1039/c0xx00000x

www.rsc.org/xxxxxx

ARTICLE TYPE

Fabrication of ZnO nanoplates for visible light-induced imaging of living cells

Jooran Lee [a], Joon Sig Choi [b] and Minjoong Yoon*[a]

Received (in XXX, XXX) Xth XXXXXXXXX 20XX, Accepted Xth XXXXXXXXX 20XX

DOI: 10.1039/b000000x

Visible light-sensitive ZnO nanoplates (ZnO NPls) were successfully synthesized using a hydrothermal sol-gel method and their structures were characterized by using techniques such as X-ray diffraction (XRD), scanning electron microscopy (SEM), transmitting electron microscopy (TEM), atomic force microscopy (AFM) and FT-IR analysis. From these studies, the nanoplates have excellent crystallinity and perfect nanoplate morphology with diameter range from 50 nm to 250 nm and thickness of ~10nm. Surfaces of the ZnO NPls were further conjugated with hydrophilic amino groups such as aminopropyl triethoxysilane (APTES) to enhance the biocompatibility and better cell penetrations. The resultant APTES-modified ZnO NPls showed excellent colloidal stability in various aqueous media, exhibiting stable and strong red fluorescence emission (~650 nm) under visible light-excitation at 405nm. They also kept exhibiting the strong red emission even after being penetrated into living cells with negligible cytotoxicity. Therefore, the APTES-modified ZnO NPls should be promising alternative nanomaterials to the traditional quantum dots as well as previously reported ZnO cellular labelling agents which exhibit green emission by UV-excitation.

Introduction

Over the past decade, semiconductor quantum dots (QDs) [1-4] have been developed for the optical imaging of living cells to overcome two problems associated with conventional organic fluorophores[5, 6] and fluorescent proteins[7-9] - low photostability and low resolution imaging due to visible fluorescence emission masked by the cellular auto-fluorescence. The traditional QDs have very high photostability as compared to organic probes, exhibiting strong and narrow fluorescence emission peaks from visible to near infrared depending on their sizes, shapes and compositions. In general, the multi-coloured QDs can excite simultaneously using a single wavelength owing to their broader absorption band behaviours compared to organic fluorophores, which needs multiple excitation wavelengths. Thus, the QDs have been attractive for the high-resolution cellular imaging, which supports single-molecule level study of the intracellular process, tumour targeting and diagnostics by long-term *in vivo* observation of cell trafficking.[1] Nevertheless, most of the traditional QDs contain cadmium or lead which is not eco-friendly and highly toxic at the cellular levels, and their biological applications are severely limited. To overcome this problem, recently semiconductor nanoparticles have been introduced due to their biocompatibility and nontoxic nature.[10, 11] Semiconductor nanoparticles such as metal oxides and ternary I-III-VI2 chalcopyrite were extensively used for cellular imaging by modifying their surface with organic binders.[12-16] Since, these semiconductor nanoparticles are usually have hydrophobic surfaces,[14, 16] and they require additional processes for modification of the surface from hydrophobic to hydrophilic for more biocompatibility in biological applications.

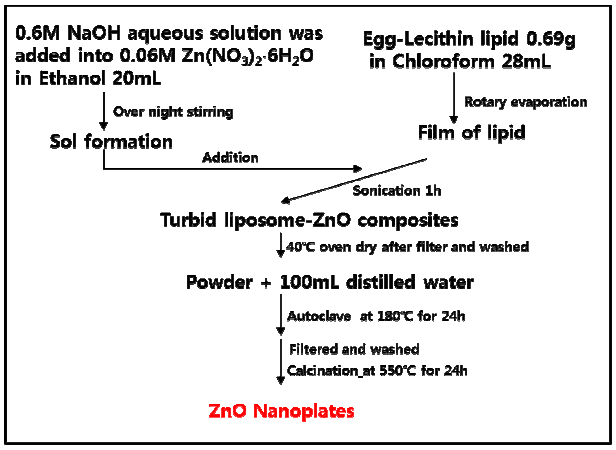

Scheme 1. Schematic flow chart for the synthesis of ZnO NPls.

Hence, ZnO nanomaterials (e.g. nanoparticles, nanorods, nanowires, nanosheets) have been attracting as alternative materials to the traditional QDs for the biological application including optical imaging of cells, because they have hydrophilic surface terminated by –OH groups.[17] Thus, recently many researchers have employed simple sol-gel methods to synthesize different biocompatible molecules-modified ZnO nanomaterials which are stable in aqueous biological medium, low toxic and highly fluorescent.[18-22] Especially ZnO nanowires and nanorods have been successfully utilized for specific cancer cell-targeted fluorescent imaging and drug loading.[18, 22] However, they absorb

only UV light region, and their biological application including the cellular imaging is still limited because biological components can be damaged not only by UV itself but also the UV-induced photocatalytic action of ZnO. Further, they emit green fluorescence (~500 nm) upon UV excitation, which can be masked by the cellular auto fluorescence. Thus, it is necessary to develop visible light-sensitive ZnO naomaterials which can emit fluorescence in the near IR region (~700 nm).

Previously, we had synthesized the visible light-sensitive ZnO nanowires by a sol-gel method through formation of liposome-ZnO nanocomposites and hydrothermal reaction, [23] and modified surface of nanowires with amino-propyl triethoxysilane (APTES). [24, 25] It was demonstrated that ZnO nanowires could deliver drugs into subcellular environments simultaneously with nanoscale optical detection of the intracellular biomolecules under visible light region. However, ZnO nanowire can be one or two in the cell by the phagocytosis process[26] because of big size (~200 nm diameter and 7-8 μm length). Particle size can affect the biodistribution and the cellular uptake pathway by influencing their adhesion and interaction with cells.[27, 28] In a recent report, particles of 100-200nm size showed a 4-fold higher rate of tumor uptake compared to particles greater than 300nm, or less than 50nm in size. [19] Therefore, ZnO nanomaterials of suitable size need to be synthesized which can uptake into cell.

Herein, we synthesized the visible light-sensitive ZnO nanoplates (NPls) which have diameter range of from 50 nm to 250 nm and ~10 nm thickness, and investigated their optical properties and visible light-induced fluorescence imaging of living cells by their surface-modification with amino-propyl triethoxysilane (APTES). [24, 25]

Experimental Section

Chemicals

The chemicals used for the synthesis of ZnO NPls were zinc nitrate hexahydrate (98%, Aldrich), egg lecithin (L-R-phosphatidyl- choline, >60%, Aldrich), chloroform (>99.8%, Samchun, Korea), sodium hydroxide (>93%, Duksan, Korea), and ethanol (200 proof, >99.8%, Aldrich). All chemicals were analytic grade reagents and used as received without further purification.

Synthesis of ZnO NPls

The schematic representation of synthesis procedure of ZnO NPls is shown in scheme 1. The ZnO NPls were synthesized using a sol-gel method which was modified from the previously reported hydrothermal reaction of liposome-ZnO composites[23]. Initially, for the preparation of ZnO NPls 100 mL of 0.6 M NaOH aqueous solution was added into 0.06 M $Zn(NO_3)_2 \cdot 6H_2O$ in ethanol (20 mL) with constant stirring under room temperature. To fabricate liposome-ZnO composites, a thin phospholipid film was prepared by evaporating the chloroform solution of egg lecithin lipid (0.025 g/mL) in a round bottom flask until dry out under reduced pressure. The lipid films were mixed with the precursory solution, followed by sonication for 60 min in an ultrasonic bath (Fisher Scientific model FS20, 70 W,42 kHz) to produce turbid liposome-ZnO composites. The turbid solution of liposome-ZnO composites were washed with distilled water and ethanol several times to remove NaOH. The collected solid matter was dispersed in 100 mL of distilled water and transferred into a Teflon-lined stainless steel autoclave maintained at 180 °C for 24 h. After the hydrothermal reaction, the Teflon-lined autoclaves were cooled naturally to room temperature. Finally, the precipitate was washed with distilled water and ethanol several times, followed by calcinations at 823 K for 24 h for the formation of nanoplates.

Surface modification of ZnO NPls

The surfaces of as-prepared ZnO NPls were modified by binding with APTES as per the previous reported.[29] In the initial step, APTES solution was prepared by dissolving 0.1% acetic acid, 4% deionized water and 2% APTES in ethanol. The ZnO NPls were dispersed in a flask (200 mL) containing 10 mL ethanol under constant ultrasonication for 30 min. And the APTES solution was added into the ethanol dispersed ZnO NPls solution and stirred for 24 h. The solution was washed with ethanol and deionized water several times using repeated centrifugation. Finally an aliquot of these particles were dried under oven at 40℃.

Structural and optical characterization techniques

Structural and morphological characterizations of the ZnO NPls were carried out using X-ray diffraction (XRD), Scanning electron microscopy (SEM), Transmission electron microscopy (TEM) and atomic force microscopy (AFM) techniques. Crystallinity and phase purity of the as-prepared nanoplates were characterized by measuring XRD, using a rotating anode X-ray diffractometer (D/MAX-2200 Ultima/PC) with Cu K α radiation (λ) 1.5405 Å). The SEM images were recorded using JSM electron microscope (JEOL; JSM-7000F). TEM images were carried out by using a transmission electron microscope (JROL-1200 EX). The sample solution was prepared by treating the above synthesized ZnO NPls in anhydrous ethanol followed by sonication for 10 min. A drop of the resultant mixture was drop casted over a TEM grid (carbon Formvar-coated copper grid) and dried in room temperature. The AFM measurements were carried out in a humidity-controlled box equipped with an AFM (METRIS-2000, Burleigh Instrument, USA). The functional groups and vibrational assignments of the APTES-ZnO NPls were investigated by FT-IR analysis. The FT-IR spectra were recorded with the KBr pellet technique using a JASCO FT-IR 4100 spectrometer.

For the optical properties, diffuse reflectance UV-vis absorption spectra were recorded using a Shimadzu UV-3101PC spectrophotometer equipped with an integral sphere. The steady state fluorescence spectra were obtained at room temperature with visible light at 410 nm, using a Ti:sapphire laser (Coherent model Mira 900) under second harmonic generation.

The particle sizes and zeta potentials of the dispersed solution of ZnO NPls and APTES-ZnONPls were measured respectively by dynamic light scattering (DLS) and laser doppler velocimetry (LDV) using a electrophoretic light scattering spectrophotometer (Otsuka electronics co, ltd; ELS-Z2).

Cell culture

As living cells, HeLa cells were grown in 89% Dulbecco's modified Eagle's medium (DMEM) with 10% fetal bovine serum and 1% antibiotic-antimycotic solution. Cells were routinely maintained on plastic tissue culture dishes at 37℃ in a humidified 5% CO_2/95% air-containing atmosphere.

Laser scanning confocal microscopy (LSCM)

The cell proliferation was analysed frequently and the cells were seeded in tissue culture dishes. The cells were treated with 10 µg/mL APTES-ZnO NPls for 24 h under controlled condition. The fluorescence images of the intracellular APTES-ZnO NPls were observed by LSCM (LSM5 Live configuration vario two VRGB) under visible light region at 405 nm.

Evaluation of cytotoxicity

The cytotoxicity of the injected ZnO NPls were evaluated using 3-(4,5-dimethylthiazol-2yl)-2,5-diphenyl-2H-tetrazolium bromide (MTT) assay. MTT solution was dissolved in Dulbecco's phosphate buffered saline (DPBS) at 2 mg/mL just before use and filtered through 0.22 µm polycarbonate membrane filters for sterilization to remove the small amount of insoluble residue present in some batches of MTT. HeLa cells or were seeded at a density of $2x10^4$cells/well in 96 well microassay plates and were incubated for 24h at 37 ℃ under a 5% CO_2 atmosphere. After incubation, the cells were treated with the APTES-ZnO NPls as well as polyethyleneimine (PEI) 25 kDa as the internal standard at various concentrations for 24h at 37 ℃ under humidified atmosphere (5% CO_2 + 95% air). The 26 µL of 2 mg/mL MTT stock solution in DPBS was then added and the plates were incubated for an additional 4 h at 37 ℃. Then, the MTT-containing medium was aspirated off and 150 µL of DMSO was added inorder to dissolve the formazan crystal formed by living cells. The absorbance was measured at 570 nm using a microplate reader (VersaMax, Molecular Devices, US). The cell viability (%) was calculated by the following equation: Cell viability (%) = ($OD_{570(sample)}$/$OD_{570(control)}$) x 100.

Results and discussion

Fig. 1 shows the XRD patterns of the as-prepared ZnO NPls. The diffraction pattern shows the hexagonal wurtzite phase of the ZnO structure of crystallization as reported in the standared JCPDS card (JCPDS 05-0664). The sharp and high intense peak demonstrates the excellent crystalline nature of the sample. From the diffraction pattern, no characteristic peaks of other phases were observed, indicating that the ZnO precursors grew into pure ZnO single crystalline structures without any lipid contamination. The SEM (Fig. 2A) and TEM images (Fig. 2B (a) and (b)) of the as-synthesized ZnO NPls exhibit the plate-like morphology. In addition to this, the morphology of the ZnO NPls were observed more specifically using tapping-mode AFM. For AFM analysis the sample was prepared by coating a few drop of well dispersed nanoplates solution on a cover glass plate. Fig. 3 shows the resultant AFM images of the ZnO NPls. The size distribution seems to be the same as that observed through SEM and TEM analysis, exhibiting the nanoplates of diameter ranging from 50 nm to 250 nm with ~10nm thickness. These results confirm that the synthesized ZnO nanostructures are actually two-dimensional nanoplate structures of appropriate size for the high rate of

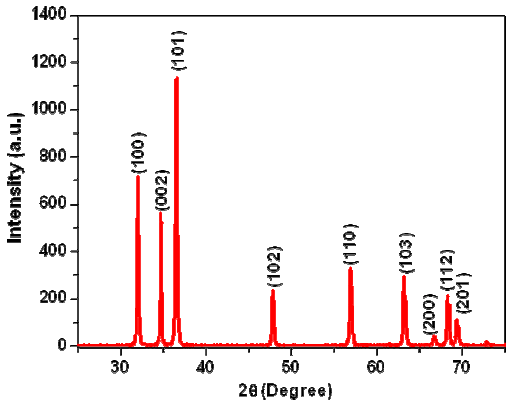

Fig. 1 X-ray diffraction pattern of ZnO NPls.

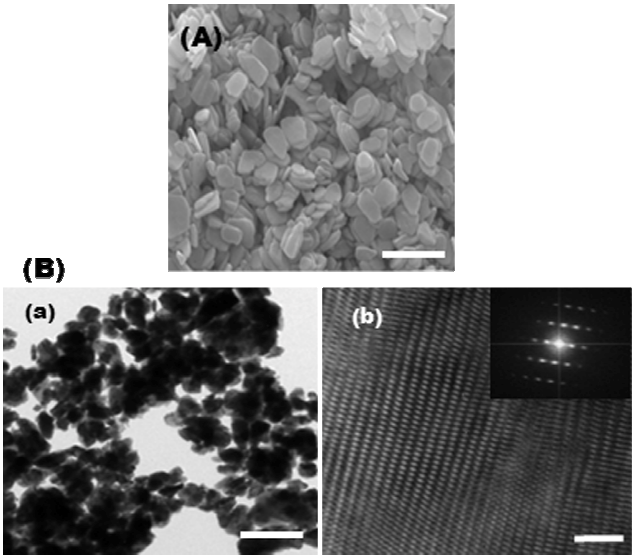

Fig. 2 (A) SEM and (B) TEM images of ZnO NPls. Inset in (b): Fast Fourier Transform (FFT) of the corresponding structures. The size of scale bars in (A, a) and (b) are 500 nm and 1 nm, respectively.

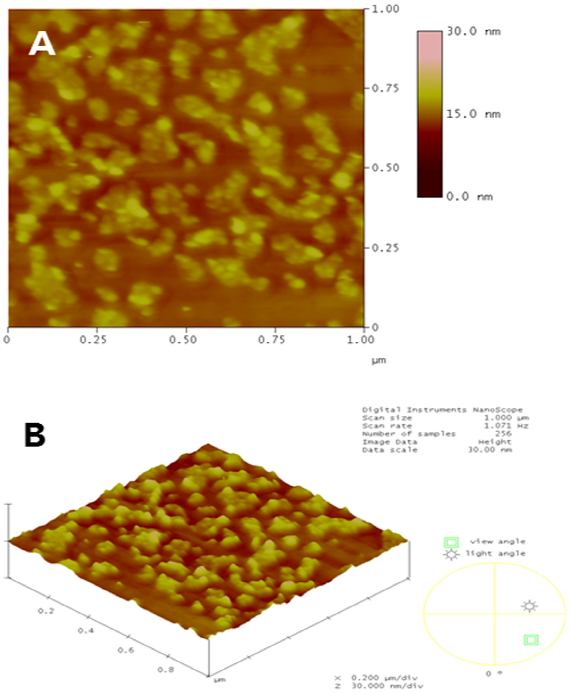

Fig. 3 Tapping-mode AFM image of ZnO NPls on cover glass, (A) 2D and (B) 3D, exhibiting nanoplates morphology.

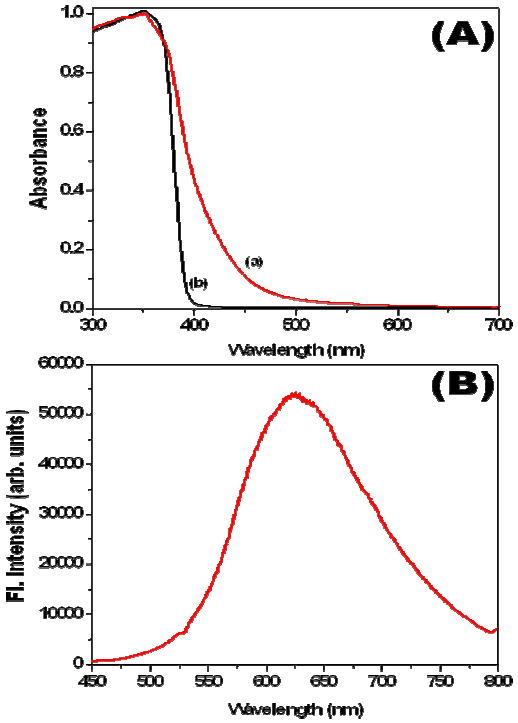

Fig. 4 (A) UV-visible absorption spectra (A) and (B) fluorescence emission spectra of ZnO NPls (a) and ZnO nanoparticles (b). Excitation wavelength was visible light region at 410nm using a Ti/sapphire laser.

tumour cell uptake.[19]

Fig. 4A (a) shows the diffuse reflectance UV-visible absorption spectra of the as-prepared ZnO NPls measured at room temperature. It exhibits broad visible light-surface absorption band from 400 nm to 580 nm, which is much red-shifted as compared to UV exciton absorption of ZnO nanoparticles (Fig. 4A (b)). Accordingly, the powder of ZnO NPls shows a broad and red fluorescence emission band around 620nm with visible light excitation at 410 nm (Fig. 4B). The red emission, which is commonly referred as a deep-level or trap-state emission,[23] is originated from radiative recombination of a photogenerated hole with an electron occupying the oxygen vacancy. These results indicate that ZnO NPls can be used as the visible light-induced fluorescence probe of the cellular imaging.

For the efficient targeting and penetration of the NPls into living cells, the ZnO NPls were conjugated with APTES. The existence of functional groups of APTES over the ZnO NPls was analysed using FT-IR spectroscopy. The FT-IR spectra of the purified APTES-ZnO NPls and ZnO NPls are shown in Fig. 5 (A). The FT-IR spectra of the ZnO NPls were recorded in the KBr phase in the frequency range between 400 cm^{-1} – 4000 cm^{-1}. The recorded FT-IR spectra were compared and indexed with the standard spectra of the functional groups. The Zn-O stretching vibrational bands were observed at about 470 cm^{-1} for both APTES-ZnO NPls and naked ZnO NPls. However, N-H stretching vibration band around 3250 cm^{-1}, symmetric and asymmetric C-H stretching vibration band at 2933 cm^{-1} and 2884 cm^{-1}, Zn-O-Si and Si-O-Si symmetrical stretching vibration band at 1108 cm^{-1} and 1012 cm^{-1} observed only from APTES-ZnO NPls (Fig. 5A(a)). These facts indicate that the aminosilane ligands (APTES) were bound on the surface of ZnO NPls through

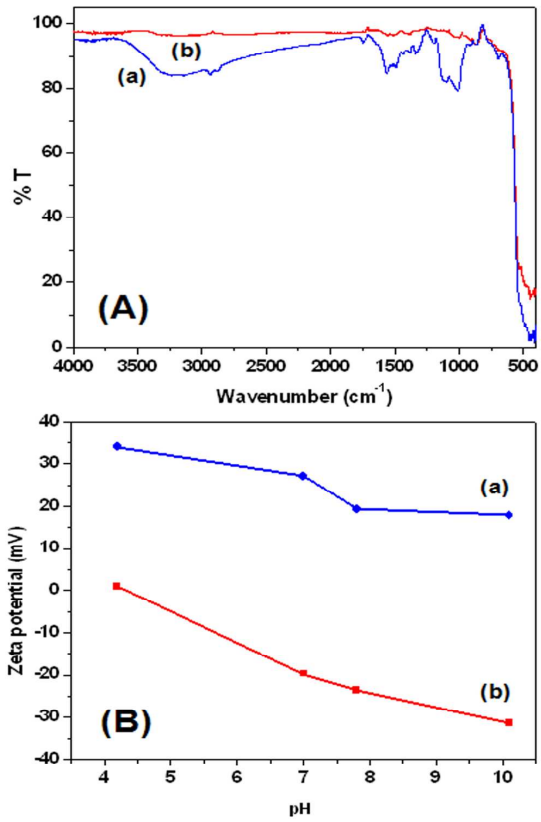

Fig. 5 (A) FT-IR spectra (a) APTES-ZnO NPls and (b) ZnO NPls and (B) corresponding zeta potential measurements against pH of the suspension.

covalent chemical bonds.

The surface functionality of APTES-ZnO NPls and ZnO NPls was also examined by zeta potential measurements as a function of suspension pH (Fig. 5B and Fig. S1). The naked ZnO NPls was observed to be strongly negative charged as proved by zeta potential of -21.6 mV at pH 7.4 in buffer which is the same as the culture medium of cells. On the contrary, APTES-ZnO NPls in the same buffer solution showed large positive zeta potential of +20.4 mV, indicating that the surface of ZnO NPls was significantly changed due to ionization of $–NH_2$ groups of APTES to $–NH_3^+$.[18, 29] The large zeta potentials also imply that APTES-ZnO NPls is stable with minimum aggregation in the pH 7.4 suspensions. Actually the dynamic light scattering (DLS) measurements showed that APTES-ZnO NPls of 1 mg/ml in pH 7.0 deionized water were found to have average diameter of 400 nm which is much smaller than that of pure ZnO nanoparticles (990 nm) (see Fig. S2, Fig. S3 and Fig. S4). Such large positive charge and well dispersion properties of APTES-ZnO NPls in the pH condition of cell culture medium can ensure the efficient targeting and penetration of ZnO NPls into the living cells with negatively charged surfaces.[24, 30, 31]

As for the optical properties of APTES-ZnO NPls dispersed in deionized water, they exhibited the same visible light absorption band as well as a broad red fluorescence emission band around 620 nm with visible light excitation as that of ZnO NPls as shown in Fig. S5. Further the fluorescence emission was observed to be very stable in the aqueous solution without quenching for at least 7 days, implying that the particle sizes and morphology of the

NPls are not changed. The fluorescence quantum yield (Fig. S6) of APTES-ZnO NPls was determined to be 53% using a solution of Rhodamin B in ethanol (QY = 65%) as the reference material,[32] indicating that APTES-ZnO NPls can be useful fluorescence probe in the aqueous medium.

As for the cytotoxicity of APTES-ZnO NPls, viability of HeLa cells was measured after 24 hr-incubation of the cells with different concentrations of the NPls. As shown in Fig. 6. Viability of the cells was observed to be remaining strong and better than 90% even with high concentration of the NPls (90 µg/mL). From this cytotoxicity test result, it is clear that the obtained APTES-ZnO NPls are potential candidate for biological applications.

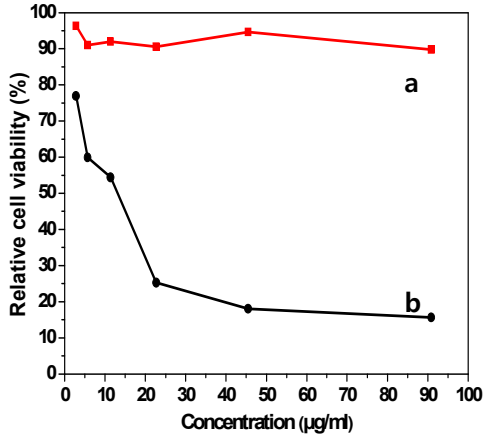

Fig. 6 Effect of APTES-ZnO NPls on cell viability. (a) APTES-ZnO NPls and (b) PEI25KDa in HeLa cells.

Finally, in order to confirm the potential cellular imaging probe of the APTES-ZnO NPls, HeLa cells were incubated with 10 µg/mL APTES-ZnO NPls in a petri dish for 24 h, followed by measuring confocal fluorescence with visible light excitation at 405 nm using LSCM system. Fig. 7A shows the red fluorescence image of APTES-ZnO NPls dispersed in the cell culture medium, exhibiting well dispersion of the nanoplates. After incubation with HeLa cells, most of the nanoplates were observed to be penetrated into the cells as shown by their red fluorescence images in the cells (Fig. 7B) which were clearly comparable to the DIC (Fig. 7C) and merge (Fig. 7D) images. It is noteworthy that the red fluorescence image was observed to be highly resolved without overlapping with the auto-fluorescence image of HeLa cells (Fig. S7). Interestingly careful examination of the fluorescence images of the NPls in not only HeLa cells but also HEK 293 cells (Fig. S8) indicate that the size and structure of the NPls remain constant during the intracellular uptake process. These results demonstrate that the cells could be effectively probed with the APTES-ZnONPls through visible light-induced red fluorescence imaging, which in turn proved that APTES-ZnO NPls could serve as alternative materials to the traditional QDs and the existing ZnO cellular labelling agents which exhibit green emission by UV-excitation.

Conclusions

Visible light-sensitive ZnO NPls were successfully synthesized using a hydrothermal synthesis method and modified with

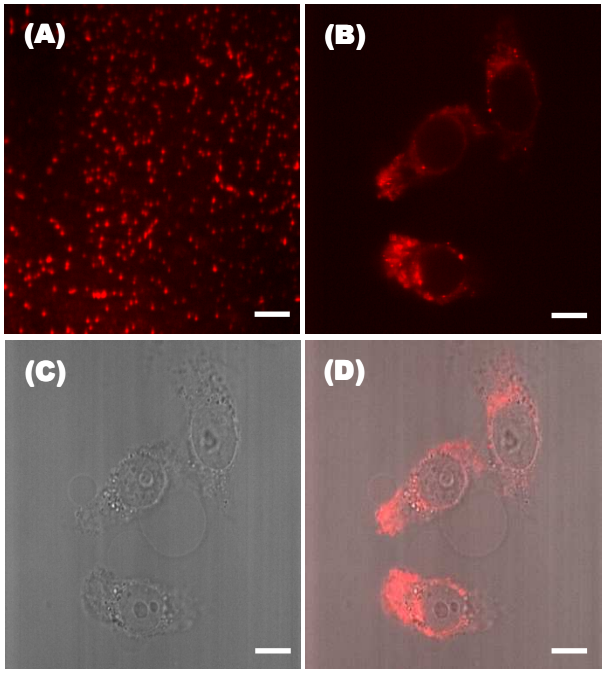

Fig. 7 Confocal fluorescence images of (A) free APTES-ZnO NPls and (B) APTES-ZnO NPls in HeLa cells under visible light of 405nm as compared with (C) DIC image and (D) merge image of HeLa.

hydrophilic amino groups on the surfaces. Synthesized ZnO NPls have high crystallinity with diameter range from 50nm to 250nm and thickness in 10nm. The APTES-modified ZnO NPls showed excellent cellular uptake followed by strong red emission under visible light excitation with low cytotoxicity, which avoids overlap with the green auto-fluorescence of cells. Therefore, the synthesized ZnO NPls would be alternative nanomaterials to the traditional semiconductor quantum dots for the future biocompatible and visible light-induced cellular imaging applications.

Acknowledgements

This work was supported by the National Research Foundation of Korea (Project number: NRF 2012R1A1A 2039168) and Chungnam National University (2011 research fund).

Notes and references

[a] *Molecular/Nano Photochemistry and Photonics Lab, Department of Chemistry, Chungnam National University, Daejeon 305-764, South Korea, Fax: +82-42-823-7008; Tel: +82-42-821-6546; E-mail: mjyoon@cnu.ac.kr*

[b] *Department of Biochemistry, Chungnam National University, Daejeon 305-764, South Korea*

† Electronic Supplementary Information (ESI) available: additional data with zeta potential measurement, particle size measurement using DLS and PL mesurement. See DOI: 10.1039/b000000x/

1 X. Michalet, F. F. Pinaud, L. A. Bentolila, J. M. Tasy, S. Doose, J. J. Li, G. Sundaresan, A. M. Wu, S.S. Gambhir and S. Weiss, Quantum dots for live cells, *in vivo* Imaging, and diagnostics, *Science*, 2005, **307**, 538-544.

2 W. C. W. Chan and S. Nie, Quantum Dot Bioconjugates for Ultrasensitive Nonisotopic Detection, *Science*, 1998, **281**, 2016-2018.

3 V. Biju, D. Muraleedharan, K. Nakayama, Y. Shinohara, T. Itoh, Y. Baba and M. Ishikawa, Quantum dot-insect neuropeptide conjugates for fluorescence imaging, transfection, and nucleus targeting of living Cells, *Langmuir*, 2007, **23**, 10254-10261.

4 W. A. Hild, M. Breunig and A. Goepferich, Quantum dots-Nano-sized probes for the exploration of cellular and intracellular targeting, *Eur. J. Pharmaceut. Biopharmaceut.*, 2008, **68**, 153-168.

5 M. Roederer, A. B. Kantor, D. R. Parks and L. A. Herzenberg, Cy7PE and Cy7APC: Bright New Probes for Immunofluorescence, *Cytometry*, 1996, **24**, 191-197.

6 P. C. Hickey, S. R. Swift, M. G. Roca and N. D. Read, Live-cell Imaging of Filamentous Fungi Using Vital Fluorescent Dyes and Confocal Microscopy, *Methods Microbiol.*, 2004, **34**, 63-67.

7 T. Nagai, K. Ibata, E. S. Park, M. Kubota, K. Mikoshiba and A. Miyawaki, A variant of yellow fluorescent protein with fast and efficient maturation for cell-biological applications, *Nature Biotechnol.*, 2002, **20**, 87-90.

8 E. Betzig, G. H. Patterson, R. Sougrat, O. W. Lindwasser, S. Olenych, J. S. Bonifacino, M. W. Davidson, L. Jennifer and H. F. Hess, Imaging intracellular fluorescent proteins at nanometer resolution, *Science*, 2006, **313**, 1642-1645.

9 P. Varnai and T. Balla, Live cell imaging of phosphoinositide dynamics with fluoresent protein domains, *Biochim. Biophys. Acta*, 2006, **1761**, 957-967.

10 K. T. Thurn, E. M. B. Brown, A. Wu, S. Vogt, B. Lai, J. Maser, T. Paunesku and G. E. Woloschak, Nanoparticles for applications in cellular Imaging, *Nanoscale Res Lett*, 2007, **2**, 430-441.

11 S. Jiang, M. K. Gnanasammandhan and Y. Zhang, Optical imaging-guided cancer therapy with fluorescent nanoparticles, *J. R. Soc. Interface*, 2010, **7**, 3-18.

12 X. Tang, W. Cheng, E. S. G. Choo and J. Xue, Synthesis of CuInS2-ZnS alloyed nanocubes with high luminescence, *Chem. Commun.* 2011, **47**, 5217-5219.

13 T. Torimoto, S. Ogawa, T. Adachi, T. Kameyama, K. Okazaki, T. Shibayama, A. Kudo and S. Kuwabata, Remarkable photoluminescence enhancement of ZnS-AgInS2 solid solution nanoparticles by post-synthesis treatment, *Chem. Commun*. 2010, **46**, 2082-2084.

14 Y. Sheng, X. Tang and J. Xue, Synthesis of AIZS@SiO_2 core-shell nanoparticles for cellular imaging applications, *J. Mater. Chem*., 2012, **22**, 1290-1296.

15 K. Yong, I. Roy, R. Hu, H. Ding, H. Cai, J. Zhu, X. Zhang, E. J. Bergey and P. N. Prasad, Synthesis of ternary $CuInS_2$/ZnS quantum dot bioconjugates and their applications for targeted cancer bioimaging, *Integr. Biol.*, 2010, **2**, 121-129.

16 X. Tang, K. Yu, Q. Xu, Qinghua; E. S. G. Choo,G. K. L. Goh and J. Xue, Synthesis and characterization of AgInS2-ZnS heterodimers with tunable photoluminescence, *J. Mater. Chem.* 2011, **21**, 11239-11243.

17 A. Abdolmaleki, S. Mallakpour and S. Borandeh, Preparation, characterization and surface morphology of novel optically active poly(ester-amide)/functionalized ZnO bionanocomposites via ultra-sonication assisted process, *Applied Surface Science*, 2011, **257**, 6725-6733.

18 S. Mitra, B. Subia, P. Patra, S. Chandra, N. Debnath, S. Das, R. Banerjee, S. C. Kundu, P. Pramanik and A. Goswami, Porous ZnO Nanorod for Targeted Delivery of Doxorubicin: *in vitro* and *in vivo* Response for Therapeutic Applications, *J. Mater. Chem.* 2012, **22**, 24145-24154

19 J. W. Rasmussen, E. Martinez, P. Louka and D. G. Wingett, Zinc oxide nanoparticles for selective destruction of tumor cells and potential for drug delivery applications, *National Institutes of Health Public Access*, 2010, **7**, 1063-1077.

20 H. J. Zhang, H. M. Xiong, Q. G. Ren, Y. Y. Xia and J. L. Kong, ZnO@silica core-shell nanoparticles with remarkable luminescence and stability in cell imaging, *J. Mater. Chem.*, 2012, **22**, 13159-13165.

21 H. M. Xiong, Y. Xu, Q. G. Ren and Y. Y. Xia, Stable aqueous ZnO@Polymer core-shell nanoparticles with tunable photolumi-nescence and their application in cell imaging, *J. Am. Chem. Soc*., 2008, **130**, 7522-7523.

22 H. Hong, J. Shi, Y. Yang, Y. Zhang, J. W. Engle, R. J. Nickles, X. Wang and W. Cai, cancer-targeted optical imaging with fluorescent zinc oxide nanowires, *Nano Lett.*, 2011, **11**, 3744-3750.

23 J. Lee and M. Yoon, Synthesis of visible light-sensitive ZnO nanostructures: Subwavelength waveguides, *J. Phys. Chem. C*, 2009, **113**, 11952-11958.

24 L. Nie, L. Gao, P. Feng, J. Zhang, X. Fu, Y. Liu, X. Yan and T. Wang, Three-dimensional functionalized tetrapod like ZnO nanostructures for plasmid DNA delivery, *Small*, 2006, **2**, 621-625.

25 J. Lee, S. Choi, S. J. Bae, S. M. Yoon, J. S. Choi and M. Yoon, Visible light-sensitive APTES-bound ZnO nanowire toward a potential nanoinjector sensing biomolecules in a living cell, *Nanoscale*, 2013, **5**, 10275-10282

26 Z. Li, R. Yang, M. Yu, F. Bai, C. Li and Z. L. Wang, Cellualr level biocompatibility and biosafety of ZnO nanowires., *J. Phys. Chem. C.*, 2008, **112**, 20114-20117.

27 K. Shapero, F. Fenaroli, I. Lynch, D.C. Cottell, A. Salvati and K. A. Dawson, Time and space resolved uptake study of silica nanoparticles by human cells., *Mol Biosyst.* 2011, **7**, 371-378.

28 I. Rivolta, The effect of nanoparticle uptake on cellular behavior: disrupting or enabling functions?, *Nanotechnology, Science and Applications.*, 2012,**5**, 87-100.

29 Y. Zhang, H. Wu, X. Huang, J. Zhang and S. Guo, Effect of Substrate (ZnO) Morphology on enzyme immobilization and its Catalytic activity, *Nanoscale Research Letters*, 2011, **6**, 450-456.

30 B. R. McNaughton, J. J. Cronican, D. B. Thompson and D. R. Liu, Mammalian cell penetration, siRNA transfection, and DNA transfection by supercharged proteins, *Proc. Natl. Acad. Sci.*, 2009, **106**, 6111-6116.

31 T. Iversen, T. Skotland and K. Sandvig, Endocytosis and intracellular transport of nanoparticles: Present knowledge and need for future studies, *Nano Today*, 2011, **6**, 176-185.

32 A. Mahasin F, A. Israa F and A. Ali Abid D, Analysis of the effect of the concentration of Rhodamine B in ethanol on the fluorescence spectrum using the "Gauss Mod" function, *J. Phys. Sci.,* 2011, **22**, 77-86.

Table of Contents

Fabrication of ZnO nanoplates for visible Light-induced imaging of a living cell

Jooran Lee[a], *Joon Sig Choi*[b] *and Minjoong Yoon**[a]

The APTES-modified ZnO Nanoplates (NPls) showed excellent permeability into HeLa cells with negligible cytotoxicity, exhibiting strong red fluorescence emission (~650nm) under visible light excitation at 405nm. Therefore, the synthesized ZnO NPls would be useful for the highly resolved cellular imaging by avoiding the overlap with the cellular intrinsic green emission.